ERJ open research
THE BEST IN OPEN ACCESS BASIC, TRANSLATIONAL & CLINICAL RESPIRATORY RESEARCH

Early View

Original research article

Endothelial to mesenchymal transition: a precursor to pulmonary arterial remodelling in patients with idiopathic pulmonary fibrosis

Archana Vijay Gaikwad, Wenying Lu, Surajit Dey, Prem Bhattarai, Greg Haug, Josie Larby, Collin Chia, Jade Jaffar, Glen Westall, Gurpreet Kaur Singhera, Tillie-Louise Hackett, Mathew Suji Eapen, Sukhwinder Singh Sohal

Please cite this article as: Gaikwad AV, Lu W, Dey S, *et al*. Endothelial to mesenchymal transition: a precursor to pulmonary arterial remodelling in patients with idiopathic pulmonary fibrosis. *ERJ Open Res* 2023; in press (https://doi.org/10.1183/23120541.00487-2022).

Endothelial to mesenchymal transition: a precursor to pulmonary arterial remodelling in patients with idiopathic pulmonary fibrosis

Archana Vijay Gaikwad[1,2], Wenying Lu[1,2,3], Surajit Dey[1], Prem Bhattarai[1], Greg Haug[4,1], Josie Larby[4,1], Collin Chia[3,4,1], Jade Jaffar[5,6], Glen Westall[5,6], Gurpreet Kaur Singhera[7,8], Tillie-Louise Hackett[7,8], Mathew Suji Eapen[1,2#], Sukhwinder Singh Sohal[1,3#*]

[1]Respiratory Translational Research Group, Department of Laboratory Medicine, School of Health Sciences, College of Health and Medicine, University of Tasmania, Launceston, Tasmania, Australia, 7248

[2]National Health and Medical Research Council (NHMRC) Centre of Research Excellence (CRE) in Pulmonary Fibrosis, Respiratory Medicine and Sleep Unit, Royal Prince Alfred Hospital, Camperdown, NSW 2050, Australia.

[3]Launceston Respiratory and Sleep Centre, Launceston, TAS, Australia.

[4]Department of Respiratory Medicine, Launceston General Hospital, Launceston, Tasmania 7250, Australia.

[5]Department of Allergy, Immunology and Respiratory Medicine, The Alfred Hospital, Melbourne, Australia.

[6]Department of Immunology and Pathology, Monash University, Melbourne, Australia

[7]Department of Anaesthesiology, Pharmacology and Therapeutics, University of British Columbia, Vancouver, BC, Canada.

[8]Centre for Heart Lung Innovation, St. Paul's Hospital, Vancouver, BC, Canada.

#Equal contributors

***Corresponding Author**

Dr Sukhwinder Singh Sohal

Respiratory Translational Research Group

Department of Laboratory Medicine, School of Health Sciences,

College of Health and Medicine, University of Tasmania

Locked Bag – 1322, Newnham Drive

Launceston, Tasmania 7248, Australia

Telephone number: +61 3 6324 5434

Email: sukhwinder.sohal@utas.edu.au

Abstract

Background: We have previously reported arterial remodelling in patients with idiopathic pulmonary fibrosis (IPF) and suggested that endothelial to mesenchymal transition (EndMT) might be central these changes. This study aims to provide evidence for active EndMT in IPF patients.

Methods: Lung resections from thirteen patients with IPF and fifteen normal controls (NC) were immunostained for EndMT biomarkers: VE-cadherin, N-cadherin, S100A4 and vimentin. Pulmonary arteries were analysed for EndMT markers by using computer and microscope assisted image analysis software Image ProPlus7.0. All the analysis was done with observer blinded to subject and diagnosis.

Results: Increased expression of mesenchymal markers N-cadherin ($p<0.0001$), vimentin ($p<0.0001$), and S100A4 ($p<0.05$), was noted with downregulation of junctional endothelial VE-cadherin ($p<0.01$) in intimal layer of the arteries from patients with IPF compared to NC. Cadherin switch was observed in IPF patients, showing increase in endothelial N-cadherin and decrease in VE-cadherin ($p<0.01$). There was also VE-cadherin shift from junctions to cytoplasm ($p<0.01$), effecting endothelial cell integrity in patients with IPF. In IPF, individual mesenchymal markers vimentin and N-cadherin negatively correlated with diffusing capacity of the lungs for carbon monoxide ($r'=-0.63$, $p=0.03$ and $r'=-0.66$, $p= 0.01$). Further, N-cadherin positively correlated with arterial thickness ($r'=0.58$, $p=0.03$).

Conclusion: This is the first study to demonstrate active EndMT in size based classified pulmonary arteries from IPF patients and potential role in driving remodelling changes. The mesenchymal markers had negative impact on the diffusing capacity of the lungs for carbon monoxide. This work also informs early origins of pulmonary hypertension in patients with IPF.

Key Words

Idiopathic pulmonary fibrosis, Pulmonary hypertension, Pulmonary artery, Vascular remodelling and Endothelial to mesenchymal transition

Introduction

Idiopathic pulmonary fibrosis is a highly progressive lung disease with limited therapeutic options (1). Although unknown causes, the current IPF pathophysiology emphasises the critical role of alveolar epithelial injury, followed by an aberrant wound healing process resulting in fibrosis and destructive lung scarring (1, 2). Fibrosis of the lung restricts efficient gas exchange, effectively inducing systemic hypoxic conditions and death due to oxygen deficiency. Similar to the epithelial injury, alterations to pulmonary vasculature also occur, resulting in abnormal vascular remodelling (3). The modification to the vascular structure includes proliferative intima, thickening of the medial smooth muscle layer, plexiform lesions and complete occlusion or narrowing of the vessels by scarred tissues (1, 3-5). Such vascular remodelling can lead to pulmonary hypertension (PH), comorbidity that frequently complicates IPF pathology and worsens prognosis, especially in late stage of the disease (6, 7).

Recent findings suggest the active involvement of several cells in IPF. However, cells vulnerable to transition under pathological conditions, such as airway basal epithelial, alveolar type II pneumocytes, macrophages and pulmonary endothelial cells, are crucial contributors to tissue fibrosis (8, 9). The transition of endothelium occurs through endothelial-to-mesenchymal transition (EndMT), which is a critical mechanism in vascular remodelling that can further progress to fibrotic alterations (10-12). EndMT induced vascular changes are reported in IPF (1, 13, 14), intestinal fibrosis (15) and cardiac fibrosis (16). Our recent study has found that arterial wall thickening, luminal occlusion, and disruptive extracellular matrix (ECM) deposition occurs in IPF patients, and EndMT possibly drive these changes (3). However, the contribution of EndMT to vascular remodelling and its association with lung fibrosis in IPF patients is poorly defined. In EndMT, loss of junctional proteins such as vascular endothelial cadherins (VE-cadherins) and gain of migratory mesenchymal traits occur. The increase in endothelial expression of mesenchymal proteins such as N-cadherin, S100A4 and vimentin are suggestive of endothelial to mesenchymal transitions (17, 18).

This study investigates EndMT as a dynamic process in relation to vascular remodelling in IPF by analysing the EndMT biomarkers. We performed a quantitative assessment of endothelial junctional marker VE-cadherin and mesenchymal markers S100A4, vimentin and N-cadherin protein levels in the classified pulmonary arteries from patients with IPF and

compared them with normal controls. Furthermore, we analysed the correlations between the mesenchymal markers, arterial remodelling, and lung function parameters.

Introduction Material and methods

Study population

Surgically resected human lung tissues from thirteen patients with IPF were obtained from Alfred Health Biobank Melbourne (Alfred Health Biobank Melbourne, ethics ID: 336-13). None of the patients were on any antifibrotic medication, and all had pathologist-verified histopathology reports of Usual Interstitial Pneumonia (UIP). Fifteen healthy normal control (NC) subjects, comprising small airways and parenchymal areas (ethics ID: H00-50110), were provided from James Hogg Lung Registry, University of British Columbia. Detailed subject demographics are provided in Table 1.

Immunohistochemical staining for EndMT markers

The lung tissue resections were deparaffinised using xylene and ethanol. Following antigen retrieval using a Decloaking Chamber (Biocare Medical, Pacheco, CA) at 110 °C for 15 minutes with target retrieval citrate buffer pH 6.0 (Dako S2369) and at 95 °C for 15 minutes with retrieval buffer pH 9.0 (Dako S2367) respectively. The tissues were stained with EndMT primary antibodies, polyclonal rabbit anti-human S100A4 (1:1000; Dako A5114), VE-cadherin (CD144) mouse monoclonal (1:150; Thermofisher 14144982), vimentin mouse monoclonal (1:200; Dako, M7020), and mouse monoclonal anti-N cadherin (1:100; Abcam Ab98952) for 60 minutes; with inflammatory markers, including mouse anti-human CD4 (1:50, Dako, M7310), mouse anti-human CD8 (1:50, Leica Biosystems, NCL-CD8-4B11-L-CE), CD68 (1:100, Dako, M0814), mouse anti-human neutrophil elastase (NE, 1:200, Dako, M0752), and mouse monoclonal mast cell chymase (CMA1, 1:100, Abcam, ab2377); and with the pericyte marker platelet-derived growth factor receptor-β (PDGFR-β, 1:100, LSBio, LS-C150026); followed by secondary HRP rabbit/ mouse antibodies (Dako K5007). The protein markers were visualised as brown with the addition of DAB substrate (Dako K5007). The nucleus was counterstained with Hematoxylin (Australian Biostain P/L).

Measurement strategies for pulmonary arteries

Arterial images were acquired from NC and patients with IPF by using a 4x objective in a vertical uni-direction to avoid overlap using. We used a Leica DM 500 microscope with attached Leica IC50W digital camera for analysis. Using measuring tools from the ProPlus

7.0 program, the external length (one end to the other end of adventitia) for pulmonary arteries were measured. These measurements were used for arterial classification in six groups: 100-1000µm (interspaced 100 or 200µm), similar to the strategy used in our earlier study (3).

VE-cadherin and N-cadherin expression in the basement membrane of pulmonary arteries

We used different magnifications to capture images across all arterial sizes. For example, smaller arteries 100-199µm- 63x objective, for 200-399µm and 400-599µm - 40x objective while larger arteries 600-1000µm- 20x objective, respectively. Further, per arterial size and subject, five images were randomly selected using an online random number generator for both VE-cadherin and N-cadherin. Firstly, two trace lines were drawn, one at the basement membrane and another one at the outer endothelium as the reference using the imaging software. The average distance between the trace lines was calculated for basement membrane length using the automated program of tissue image analysis software Image-Pro Plus v7. Further, cells which stained positive (in brown colour) for junctional and cytoplasmic VE-cadherin in the reference basement membrane area were counted (Supplementary Figure 1a). Likewise, cells which stained positive (in brown colour) for junctional and cytoplasmic N-cadherin in the reference basement membrane area were counted (Supplementary Figure 1b). Additionally, total cells in the basement membrane were also counted using the imaging software.

VE-cadherin junctional and cytoplasmic positive cell percentage per average basement membrane was calculated using following formula:

$$\text{VE} - \text{cadherin junctional or cytoplasmic positive cell percentage} = \left(\frac{\text{number of positive expression cell}}{\text{Average length of basment membrane}}\right) X100$$

Similarly, N-cadherin junctional and cytoplasmic positive cell percentage per average basement membrane was calculated using following formula:

$$\text{N} - \text{cadherin junctional or cytoplasmic positive cell percentage} = \left(\frac{\text{number of positive expression cell}}{\text{Average length of basment membrane}}\right) X100$$

Pulmonary total arterial layer expression for vimentin, N-cadherin and S100A4

Image acquisition and randomisation were followed in the same way as VE-cadherin and N-cadherin cell percentage measurements. For total arterial expression for each mesenchymal (vimentin, N-cadherin and S100A4 expression), an area of interest (AOI) from the start of the outer end of the intima facing the lumen to the outer border of adventitia was manually selected using imaging software. Subsequently, mesenchymal staining colour (brown) and total dark objects from the AOI was counted using image ProPlus 7.0 software. A similar strategy was used for individual layers intima, media, and adventitia. For intimal layer mesenchymal marker expression, the outer luminal to the inner elastin layer was selected as the AOI, while for the medial mesenchymal marker expressions the external outline of the inner elastin membrane and internal lining of the external elastin membrane of the atrial smooth muscle layer was considered. The areas bordering the external elastin to the arteries outermost connective tissue were considered as adventitia for the mesenchymal marker expression measurements (Supplementary Figure 1c). Percentage of vimentin, N-cadherin and S100A4 expression was calculated using the following formula.

$$\text{Each layer percentage of mesenchymal markers expression} = \left(\frac{\text{number of selected colour objects from AOI}}{\text{total number of the dark object from AOI}}\right) X100$$

Correlations between the mesenchymal marker expression and vascular remodelling changes

Our group has previously published the study on morphometric assessment of vascular remodelling changes observed among IPF patients (3, 19). Here, we used same morphometric assessment data for correlation purposes since the patient's cohort was same. The correlation between each mesenchymal marker expression and arterial remodelling changes was performed to understand impact of EndMT.

Statistical analysis

All cross-sectional data were tested for their normal distributions using the D'Agostino-Pearson omnibus normality test. Analyses of variance was performed using ordinary one-way ANOVA using Bonferroni multiple comparison tests, which compared mean and standard deviation across all the groups of interest; specific group differences with correction for multiple comparisons were assessed using Dunn's test. Finally, for correlations, we

performed regression analyses using Pearman's rank test. All analysis was done using GraphPad prismV9, with a p-value ≤ 0.05 being considered significant.

Results

The pulmonary arteries from IPF patients exhibited notable morphological changes such as endothelial proliferation penetrating the lumen, muscular hypertrophy both in intima and medial layer and plexiform lesions compared to arteries from NC. Cytoplasmic endothelial cell expression was observed for VE-cadherin in tissue sections from patients with IPF while junctional expression was observed in NC (Figure 1A). Across all arterial sizes, mesenchymal protein N-cadherin expression was observed in all layers of classified arteries in IPF, however not seen in NC (Figure 1B). Strong vimentin and S100A4 staining were seen in all layers in IPF compared to NC. Vimentin expression was predominantly observed in the smaller and medium-sized arteries (Figure 1C). S100A4 staining was prominently seen in the intima compared to media and adventitia across all arterial ranges in IPF patients. Comparatively there was lesser S100A4 staining than vimentin and N-cadherin expression across all arterial sizes in IPF (Figure 1D).

Endothelial VE-cadherin and N-cadherin cellular expression in IPF

We assessed differential counts for VE and N cadherin in the junction and compared them with VE and N cadherin cytoplasmic expression which is presented here as the percentage of total cells in the intimal area. Endothelium of NC on average consisted of 40-50% cells that expressed junctional VE-cadherin, which drastically reduced to 5-15% in IPF ($p<0.01$), regardless of the arterial size (Figure 2A (a) and Figure 2B (a)). In addition to the loss of junctional VE-cadherin in IPF patients, we also found an incremental increase in cytoplasmic VE-cadherin which showed a fivefold increase than NC across all arterial sizes ($p<0.01$) (Figure 2A (b) and Figure 2B (b)). A larger difference in cytoplasmic VE-cadherin in IPF and NC was particularly noted for smaller arteries (range of 100-199µm) ($p<0.001$), compared to larger arteries. Interestingly we also identified close to a two-fold increase in junctional expression of N-cadherin cells across all arterial sizes ($p<0.05$) in IPF (Figure 2A (c) and Figure 2B (a)), although the cytoplasmic N-cadherin was only noticed in IPF patients and was negligible in NC (Figure 2A (d) and Figure 2B (b)).

Percent N-cadherin expression in IPF

There was significant increase in N-cadherin expression across all arterial sizes in IPF compared to NC. Total N-cadherin expression was considerably greater (4-5-fold) in IPF compared to NC across all arterial size ($p<0.0001$) (Figure 3a). Furthermore, intimal, and medial N-cadherin percent expression revealed a greater fold change compared to adventitial layer across entire arterial range in IPF (Figure 3b, c, d, and e). We found intimal and medial N-cadherin percent expression was significantly higher across all classified arterial ranges i.e.,100-1000µm ($p<0.0001$) in IPF (Figure 3b, c, d, and e). Although adventitial N-cadherin expression was less compared to media and adventitia, yet the adventitial N-cadherin expression was greatest among 200-399µm and 400-599µm ($p<0.001$) (Figure 3c, d) compared to 100-199µm ($p<0.01$) and 600-1000µm ($p<0.05$) arterial range (Figure 3b, e).

Vimentin percent expression in IPF

The total vimentin percentage significantly increased throughout the arterial ranges in IPF compared to NC ($p<0.0001$) (Figure 4a). Vimentin expression in intima and medial was significantly higher across all classified arterial ranges i.e.,100-1000µm ($p<0.0001$) in IPF (Figure 4b, c, d, and e). Increase in vimentin expression was also noted in adventitial layer for all arterial sizes. This was highly significant for arterial range of 200-599µm ($p<0.001$) (Figure 4b, c, d, e).

S100A4 percent expression in IPF

Compared to NC, total percentage staining for S100A4 was significantly higher in smaller and medium sized arteries in IPF [100-199µm ($p<0.0001$) and 200-399µm ($p<0.001$)] (Figure 5a). However, in larger arteries S100A4 expression was slightly higher in IPF (10-15%) compared to NC (8-10 %) (Figure 5d and e). Intimal expression was significantly higher in smaller arteries 199µm ($p<0.0001$; Figure 5b) compared to medium range arteries 200-599µm ($p<0.001$; Figure 5c, d) in IPF. The medial and adventitial S100A4 expression did not change across arterial sizes. Overall, the smaller arteries showed more significant changes in S100A4 expression compared to medium and large sized arteries (Figure 5b, c, d, f).

Mesenchymal maker expression impacted vascular remodelling and lung physiology

There was a significant positive correlation between increased total N-cadherin and arterial thickening; ($r'=058$, $p=0.03$) (Figure 6a). Total vimentin expression showed positive association ($r'=0.37$, $p=0.13$) with increased arterial thickness (Figure 6b). Remarkably,

intimal N-cadherin and vimentin expression significantly positively corelated to both intimal (r'=0.64, p=0.01) and adventitial thickness (r'=0.63, p=0.03) (Table 2a). Total N-cadherin and vimentin expression also showed a significant negative correlation with DLCO% predicted r'=-0.66, p=0.01 and r'=-0.63, p=0.03 respectively (Figure 6c, d). We also noted that increases in Intimal N-cadherin and vimentin negatively corelated to DLCO % predicated (r'=-0.58, p=0.03; Table 2b).

Correlation between intimal junctional and cytoplasmic VE-cadherin expression and mesenchymal proteins

We identified an interesting relationship between junctional and cytoplasmic VE-cadherin expression and mesenchymal protein expression in intimal layer across classified arteries. A negative correlation between VE-cadherin junctional and mesenchymal protein vimentin, N-cadherin, and S100A4 was observed between smaller and larger arteries (Supplementary Figure 2a and d). However, the association between junctional VE-cadherin and intimal vimentin was significant among arterial size 100-199µm (r'=-0.85, p=0.001) (Supplementary Figure 2a), whereas a strong negative relationship was also seen larger arteries 600-1000µm (r'=-0.88, p=0.31) (Supplementary Figure 2d). Furthermore, the association between junctional VE-cadherin and intimal S100A4 was also negative among all arterial sizes except for 400-599µm (Supplementary Figure 2a, b, c, d).

We also observed consistent positive relationship trend between VE-cadherin cytoplasmic expression and intimal mesenchymal protein vimentin, N-cadherin and S100A4 was observed among smaller and medium-sized arteries (Supplementary Figure 2a and b). However, we could not identify a comparable pattern in larger arterial sizes (Supplementary Figure 2c and d), which might be due to the high sample size variability observed between IPF and NC.

CD4/CD8, mast cells, neutrophil, macrophage and pericyte cell expression in pulmonary arteries from patients with IPF compared to normal controls We found negative expressions of CD4, CD8, neutrophil elastase, and CMA1 for mast cells in the arterial wall of patients with IPF. CD68 (macrophage) was the only inflammatory cell type with positive staining, but more so in the lumen of the artery or adventitial layer in IPF. Intimal endothelial cells were negative for CD68. In addition, we observed positive expression for PDGFR-β, which is a marker for pericytes. We found positive staining for pericytes in the intimal layer and the surrounding tissue, but endothelial cells were negative

for this marker as shown in the inset. Staining for inflammatory markers and pericytes is shown in figure 7A and figure 7B.

Discussion

The study here, best to our knowledge, is the first description of EndMT in the arterial vasculature of patients with IPF. We have provided both qualitative and quantitative data informing EndMT marker expression across different arterial sizes and individual layers. Our study demonstrated downregulation of junctional VE-cadherin and increased cytoplasmic VE-cadherin in patients with IPF than NC. Furthermore, we showed upregulation of mesenchymal proteins N-cadherin, vimentin and S100A4 across classified arteries in IPF. The mesenchymal expression was most prominent within the intima, suggesting that endothelial transformation via EndMT is an active process in the pulmonary arteries of patients with IPF. Strong co-relations between EndMT and arterial remodelling were observed, these included arterial thickness and ECM deposition. Moreover, we found EndMT to adversely influence lung physiological parameters, especially DLCO. Our findings suggest EndMT as novel therapeutic target in IPF.

EndMT is a crucial process in developing and progressing fibrotic changes (10-12). VE-cadherin is an endothelial cell specific protein (20) that controls permeability and regulates cell motility (21). Our study noted a significant reduction of VE-cadherin expression across all arterial sizes in IPF and a concurrent increase in cytoplasmic VE-cadherin at the intimal layer across arterial sizes. Junctional to cytoplasmic VE-cadherin expression shift suggests that endothelial cell integrity is compromised in IPF favouring EndMT. Mammoto et al. (22) cultured human lung microvascular endothelial (L-HMVE) in fibronectin-coated polyacrylamide gels with different stiffness to investigate changes between mechanical interactions which could regulate vascular permeability and observed that L-HMVE cells grown on more flexible substrates appeared round, VE-cadherin-containing cell–cell junctions were disrupted, and this was associated with increased VE-cadherin staining in the cytoplasm (22).

Further, parallel to VE-cadherin expression, we observed increase in mesenchymal proteins, vimentin, S100A4 and N-cadherin in intimal layer of the arteries. Previous IPF studies have detected loss of endothelial phenotypes and acquisition of mesenchymal phenotypes but are mainly animal studies.(13, 23). In addition, previous work has suggested that the proliferation of both endothelial and smooth muscle cells that undergo phenotypic changes

via EndMT is linked to intimal remodelling and PH pathology (24). Moreover, augmented mesenchymal protein expression noted in the media and adventitia layer suggests resident cells possibly undergo mesenchymal phenotypic transformation.

N-cadherin is also expressed in mesenchymal cells, which promotes motility and invasion (25). We also discovered the augmented expression of N-cadherin junctional positive and N-cadherin cytoplasmic positive cells in the intimal layer among IPF patients. Previously, upregulated N-cadherin expression in alveolar type II cells has been observed in IPF patients and is considered a potential prognostic indicator based on N-cadherin and Ki-67 expression correlation with histological disease activity (26). Recently, Ferrell et al. also demonstrated that retention of the N-cadherin prodomain at the cell surface is a potential biomarker of pathological myofibroblasts and is linked with tissues of the heart, lung and liver fibrosis (27). Taking it together, we believe that increase in cytoplasmic VE-cadherin could lead to the overall decrease in VE-cadherin and increase in N-cadherin indicating the process of EndMT, which drives intimal remodelling changes in IPF (1, 3). Augmented mesenchymal protein expression noted in the media and adventitia layer suggests resident cells possibly undergo mesenchymal phenotypic transformation.

The remodelling changes in media and adventitia layers could be due to mesenchymal transformation of the smooth muscle cells and the adventitial fibroblast (28, 29). N-cadherin was found to be abundantly expressed in both media and adventitia layer in IPF than healthy control group. Moreover, the correlation between N-cadherin expression and vascular remodelling changes such as arterial thickness confirms increased N-cadherin expression has been associated with increased individual layer thickness, especially intimal thickness. Thus, we suggest that targeting N-cadherin could be potential strategy to reduce vascular remodelling as suggested by earlier studies (30, 31).

Vimentin, a cytoskeletal protein that is prevalent in cells of mesenchymal origin and its overexpression been linked to increased invasiveness and excessive scarring (32). Intriguingly, our study also discovered the augmented expression of vimentin expression at intima, media, and adventitia layer within different arterial sizes in IPF. Several studies have noted vimentin overexpression in IPF lungs (33-37) with high levels of the vimentin in IPF lung tissue related to disease progression (38). Moreover, a positive correlation between total vimentin expression and arterial thickness eludes their role in arterial remodelling in IPF.

Additionally, we observed that intimal vimentin expression influenced individual layer thickness, especially the intimal thickness.

S100A4 belongs to the small Ca2+-binding protein family, and it modulates cellular biological functions, such as cell motility, proliferation, and metastasis (39-41). S100A4 causes lung fibrosis by promoting the proliferation and activation of fibroblast (42-44) and increased S100A4 elevation has been proposed to contribute in the development of IPF (45-48). The S100A4 expression was significantly higher in intima layer across all arterial sizes however, we didn't find such a significant expression in media and adventitia layers.

We next investigated the relationship between VE-cadherin junctional and cytoplasmic positive expression and mesenchymal protein expression, which suggested that upregulated VE-cadherin cytoplasmic expression is associated with increased mesenchymal protein expression, especially in case of smaller and medium-range arteries. However, larger arteries didn't show similar changes, possibly due to a smaller number of larger arteries observed in fibrotic IPF lung tissue. This trend suggests increased cytoplasmic VE-cadherin expression in endothelial cells could indicate active endothelial proliferation and transition.

In assessing the impact of EndMT on lung function, the correlation between mesenchymal markers expression and lung function parameter DLCO was performed. The correlations suggested that the increase in N-cadherin and vimentin expression could negatively impact lung gas exchange capacity (DLCO) in IPF patients, indicating PH complications. Furthermore, the reduced DLCO in IPF patients has been considered as indication of concomitant PH to the underlying pulmonary fibrosis (49). Our findings fit with this theory and suggested pathology.

To further confirm our EndMT findings and cellular expression of mesenchymal markers, we also stained for inflammatory cell populations and pericytes. We found that pulmonary arteries were negative for mast cells, CD4/CD8 and neutrophils. Some positivity was observed for macrophages (CD68 positive), but mainly in the lumen or adventitial tissue. Endothelial cells were negative for CD68. We also found positive staining for pericytes, but intimal endothelial cells were negative for PDGFR-β. This shows that endothelial cells staining for mesenchymal markers are not inflammatory cells but in fact the cells undergoing EndMT. Pericytes could also be contributing to arterial remodelling in IPF in addition to endothelial cells, but this warrants further work.

This study limitation is that the number of IPF and NC samples varied for size-based comparison, as some arterial sizes were not observed in IPF. Another limitation is the un-availability of cardiac function data or a clinical diagnosis of PH for the IPF patients studied, hence, the associations between EndMT and PH could not be established. However, the positive correlation of EndMT with vascular remodelling and negative correlation with DLCO indicates possible PH in IPF patients. Further work is needed to confirm these associations. Future studies are needed to further explore these histopathological findings with relationships to transcriptomics (50).

In summary, endothelial cells acquire mesenchymal traits through EndMT in IPF patients. Significant increased mesenchymal expression in arterial layers potentially contributes to muscular arteries remodelling and drives the physiological change such as deficient oxygen absorption. Hence, our study data validated the crucial role of EndMT in IPF pathology and suggests EndMT as novel therapeutic target for preventing PH and lung fibrosis in general.

Funding: This work was supported by research grants from Clifford Craig Foundation Launceston General Hospital and Lung Foundation Australia.

Conflict of Interest Disclosure Statement

Sukhwinder Singh Sohal reports personal fees for lectures from Chiesi, travel support from Chiesi and AstraZeneca, and research grant from Boehringer Ingelheim outside the submitted work. All the other authors do not have any conflict of interest to declare.

References

1. Gaikwad AV, Eapen MS, McAlinden KD, Chia C, Larby J, Myers S, Dey S, Haug G, Markos J, Glanville AR, Sohal SS. Endothelial to mesenchymal transition (EndMT) and vascular remodeling in pulmonary hypertension and idiopathic pulmonary fibrosis. *Expert review of respiratory medicine* 2020; 14: 1027-1043.
2. Richeldi L, Collard HR, Jones MG. Idiopathic pulmonary fibrosis. *The Lancet* 2017; 389: 1941-1952.
3. Gaikwad AV, Lu W, Dey S, Bhattarai P, Chia C, Larby J, Haug G, Myers S, Jaffar J, Westall G, Singhera GK, Hackett T-L, Markos J, Eapen MS, Sohal SS. Vascular remodelling in IPF patients and its detrimental effect on lung physiology: potential role of endothelial to mesenchymal transition (EndMT). *ERJ Open Research* 2022: 00571-02021.
4. Nathan SD, Shlobin OA, Ahmad S, Koch J, Barnett SD, Ad N, Burton N, Leslie K. Serial development of pulmonary hypertension in patients with idiopathic pulmonary fibrosis. *Respiration; international review of thoracic diseases* 2008; 76: 288-294.
5. Farkas L, Gauldie J, Voelkel NF, Kolb M. Pulmonary Hypertension and Idiopathic Pulmonary Fibrosis. *American Journal of Respiratory Cell and Molecular Biology* 2011; 45: 1-15.
6. Nathan SD, Barbera JA, Gaine SP, Harari S, Martinez FJ, Olschewski H, Olsson KM, Peacock AJ, Pepke-Zaba J, Provencher S, Weissmann N, Seeger W. Pulmonary hypertension in chronic lung disease and hypoxia. *European Respiratory Journal* 2019; 53: 1801914.
7. Lettieri CJ, Nathan SD, Barnett SD, Ahmad S, Shorr AF. Prevalence and outcomes of pulmonary arterial hypertension in advanced idiopathic pulmonary fibrosis. *Chest* 2006; 129: 746-752.
8. Kinoshita T, Goto T. Molecular Mechanisms of Pulmonary Fibrogenesis and Its Progression to Lung Cancer: A Review. *Int J Mol Sci* 2019; 20: 1461.
9. Wynn TA. Integrating mechanisms of pulmonary fibrosis. *The Journal of experimental medicine* 2011; 208: 1339-1350.
10. Ursoli Ferreira F, Eduardo Botelho Souza L, Hassibe Thomé C, Tomazini Pinto M, Origassa C, Salustiano S, Marcel Faça V, Olsen Câmara N, Kashima S, Tadeu Covas D. Endothelial Cells Tissue-Specific Origins Affects Their Responsiveness to TGF-β2 during Endothelial-to-Mesenchymal Transition. *Int J Mol Sci* 2019; 20: 458.
11. Lv Z, Wang Y, Liu Y-J, Mao Y-F, Dong W-W, Ding Z-N, Meng G-X, Jiang L, Zhu X-Y. NLRP3 Inflammasome Activation Contributes to Mechanical Stretch–Induced Endothelial-Mesenchymal Transition and Pulmonary Fibrosis. *Critical Care Medicine* 2018; 46: e49-e58.
12. Piera-Velazquez S, Mendoza FA, Jimenez SA. Endothelial to Mesenchymal Transition (EndoMT) in the Pathogenesis of Human Fibrotic Diseases. *Journal of Clinical Medicine* 2016; 5: 45.
13. Hashimoto N, Phan SH, Imaizumi K, Matsuo M, Nakashima H, Kawabe T, Shimokata K, Hasegawa Y. Endothelial–Mesenchymal Transition in Bleomycin-Induced Pulmonary Fibrosis. *American Journal of Respiratory Cell and Molecular Biology* 2010; 43: 161-172.
14. Choi SH, Hong ZY, Nam JK, Lee HJ, Jang J, Yoo RJ, Lee YJ, Lee CY, Kim KH, Park S, Ji YH, Lee YS, Cho J, Lee YJ. A Hypoxia-Induced Vascular Endothelial-to-Mesenchymal Transition in Development of Radiation-Induced Pulmonary Fibrosis. *Clin Cancer Res* 2015; 21: 3716-3726.
15. Rieder F, Kessler SP, West GA, Bhilocha S, de la Motte C, Sadler TM, Gopalan B, Stylianou E, Fiocchi C. Inflammation-Induced Endothelial-to-Mesenchymal

Transition: A Novel Mechanism of Intestinal Fibrosis. *The American Journal of Pathology* 2011; 179: 2660-2673.
16. Yoshimatsu Y, Watabe T. Roles of TGF-β Signals in Endothelial-Mesenchymal Transition during Cardiac Fibrosis. *International Journal of Inflammation* 2011; 2011: 724080.
17. Eapen MS, Lu W, Gaikwad AV, Bhattarai P, Chia C, Hardikar A, Haug G, Sohal SS. Endothelial to mesenchymal transition: a precursor to post-COVID-19 interstitial pulmonary fibrosis and vascular obliteration? *European Respiratory Journal* 2020; 56: 2003167.
18. Sanchez-Duffhues G, Orlova V, ten Dijke P. In Brief: Endothelial-to-mesenchymal transition. *The Journal of Pathology* 2016; 238: 378-380.
19. Bhattarai P, Lu W, Gaikwad AV, Dey S, Chia C, Larby J, Haug G, Hardikar A, Williams A, Kaur Singhera G, Hackett TL, Eapen MS, Sohal SS. Arterial remodelling in smokers and in patients with small airway disease and COPD: implications for lung physiology and early origins of pulmonary hypertension. *ERJ Open Res* 2022; 8.
20. Lampugnani MG, Resnati M, Raiteri M, Pigott R, Pisacane A, Houen G, Ruco LP, Dejana E. A novel endothelial-specific membrane protein is a marker of cell-cell contacts. *Journal of Cell Biology* 1992; 118: 1511-1522.
21. Vestweber D, Winderlich M, Cagna G, Nottebaum AF. Cell adhesion dynamics at endothelial junctions: VE-cadherin as a major player. *Trends Cell Biol* 2009; 19: 8-15.
22. Mammoto A, Mammoto T, Kanapathipillai M, Wing Yung C, Jiang E, Jiang A, Lofgren K, Gee EPS, Ingber DE. Control of lung vascular permeability and endotoxin-induced pulmonary oedema by changes in extracellular matrix mechanics. *Nature Communications* 2013; 4: 1759.
23. Jia W, Wang Z, Gao C, Wu J, Wu Q. Trajectory modeling of endothelial-to-mesenchymal transition reveals galectin-3 as a mediator in pulmonary fibrosis. *Cell Death & Disease* 2021; 12: 327.
24. Ghigna M-R, Dorfmüller P. Pulmonary vascular disease and pulmonary hypertension. *Diagnostic Histopathology* 2019; 25: 304-312.
25. Wheelock MJ, Johnson KR. Cadherins as Modulators of Cellular Phenotype. *Annual Review of Cell and Developmental Biology* 2003; 19: 207-235.
26. Lomas NJ, Watts KL, Akram KM, Forsyth NR, Spiteri MA. Idiopathic pulmonary fibrosis: immunohistochemical analysis provides fresh insights into lung tissue remodelling with implications for novel prognostic markers. *Int J Clin Exp Pathol* 2012; 5: 58-71.
27. Ferrell PD, Oristian KM, Cockrell E, Pizzo SV. Pathologic Proteolytic Processing of N-Cadherin as a Marker of Human Fibrotic Disease. *Cells* 2022; 11: 156.
28. Kuwabara JT, Tallquist MD. Tracking Adventitial Fibroblast Contribution to Disease: A Review of Current Methods to Identify Resident Fibroblasts. *Arterioscler Thromb Vasc Biol* 2017; 37: 1598-1607.
29. Stenmark KR, Davie N, Frid M, Gerasimovskaya E, Das M. Role of the Adventitia in Pulmonary Vascular Remodeling. *Physiology* 2006; 21: 134-145.
30. Jones M, Sabatini PJB, Lee FSH, Bendeck MP, Langille BL. N-Cadherin Upregulation and Function in Response of Smooth Muscle Cells to Arterial Injury. *Arteriosclerosis, Thrombosis, and Vascular Biology* 2002; 22: 1972-1977.
31. Lyon CA, Koutsouki E, Aguilera CM, Blaschuk OW, George SJ. Inhibition of N-cadherin retards smooth muscle cell migration and intimal thickening via induction of apoptosis. *Journal of Vascular Surgery* 2010; 52: 1301-1309.

32. Li H, Chang L, Du WW, Gupta S, Khorshidi A, Sefton M, Yang BB. Anti-microRNA-378a enhances wound healing process by upregulating integrin beta-3 and vimentin. *Mol Ther* 2014; 22: 1839-1850.
33. Yang Y, Fujita J, Bandoh S, Ohtsuki Y, Yamadori I, Yoshinouchi T, Ishida T. Detection of antivimentin antibody in sera of patients with idiopathic pulmonary fibrosis and non-specific interstitial pneumonia. *Clin Exp Immunol* 2002; 128: 169-174.
34. Felton VM, Borok Z, Willis BC. N-acetylcysteine inhibits alveolar epithelial-mesenchymal transition. *American Journal of Physiology-Lung Cellular and Molecular Physiology* 2009; 297: L805-L812.
35. Pandit KV, Corcoran D, Yousef H, Yarlagadda M, Tzouvelekis A, Gibson KF, Konishi K, Yousem SA, Singh M, Handley D, Richards T, Selman M, Watkins SC, Pardo A, Ben-Yehudah A, Bouros D, Eickelberg O, Ray P, Benos PV, Kaminski N. Inhibition and Role of let-7d in Idiopathic Pulmonary Fibrosis. *American Journal of Respiratory and Critical Care Medicine* 2010; 182: 220-229.
36. Liu G, Philp AM, Corte T, Travis MA, Schilter H, Hansbro NG, Burns CJ, Eapen MS, Sohal SS, Burgess JK, Hansbro PM. Therapeutic targets in lung tissue remodelling and fibrosis. *Pharmacology & Therapeutics* 2021; 225: 107839.
37. Zhang D, Zhuang R, Li J, Lv Y, Yang X, Pan W, Zhang X. MicroSPECT Imaging-Guided Treatment of Idiopathic Pulmonary Fibrosis in Mice with a Vimentin-Targeting 99mTc-Labeled N-Acetylglucosamine-Polyethyleneimine. *Molecular Pharmaceutics* 2021; 18: 4140-4147.
38. Surolia R, Li FJ, Wang Z, Li H, Dsouza K, Thomas V, Mirov S, Pérez-Sala D, Athar M, Thannickal VJ, Antony VB. Vimentin intermediate filament assembly regulates fibroblast invasion in fibrogenic lung injury. *JCI insight* 2019; 4.
39. Grigorian M, Andresen S, Tulchinsky E, Kriajevska M, Carlberg C, Kruse C, Cohn M, Ambartsumian N, Christensen A, Selivanova G, Lukanidin E. Tumor Suppressor p53 Protein Is a New Target for the Metastasis-associated Mts1/S100A4 Protein: FUNCTIONAL CONSEQUENCES OF THEIR INTERACTION*. *Journal of Biological Chemistry* 2001; 276: 22699-22708.
40. Boye K, Mælandsmo GM. S100A4 and Metastasis: A Small Actor Playing Many Roles. *The American Journal of Pathology* 2010; 176: 528-535.
41. Li Z-H, Bresnick AR. The S100A4 Metastasis Factor Regulates Cellular Motility via a Direct Interaction with Myosin-IIA. *Cancer Research* 2006; 66: 5173-5180.
42. Xia H, Gilbertsen A, Herrera J, Racila E, Smith K, Peterson M, Griffin T, Benyumov A, Yang L, Bitterman PB, Henke CA. Calcium-binding protein S100A4 confers mesenchymal progenitor cell fibrogenicity in idiopathic pulmonary fibrosis. *The Journal of Clinical Investigation* 2017; 127: 2586-2597.
43. Li Y, Bao J, Bian Y, Erben U, Wang P, Song K, Liu S, Li Z, Gao Z, Qin Z. S100A4(+) Macrophages Are Necessary for Pulmonary Fibrosis by Activating Lung Fibroblasts. *Frontiers in immunology* 2018; 9: 1776.
44. Zhang W, Ohno S, Steer B, Klee S, Staab-Weijnitz CA, Wagner D, Lehmann M, Stoeger T, Königshoff M, Adler H. S100a4 Is Secreted by Alternatively Activated Alveolar Macrophages and Promotes Activation of Lung Fibroblasts in Pulmonary Fibrosis. *Frontiers in immunology* 2018; 9.
45. Lee J-U, Chang HS, Shim E-Y, Park J-S, Koh E-S, Shin H-K, Park J-S, Park C-S. The S100 calcium-binding protein A4 level is elevated in the lungs of patients with idiopathic pulmonary fibrosis. *Respiratory Medicine* 2020; 171: 105945.
46. Li Z, Li Y, Liu S, Qin Z. Extracellular S100A4 as a key player in fibrotic diseases. *Journal of Cellular and Molecular Medicine* 2020; 24: 5973-5983.

47. Kagimoto A, Tsutani Y, Kushitani K, Kambara T, Mimae T, Miyata Y, Takeshima Y, Okada M. Serum S100 calcium-binding protein A4 as a novel predictive marker of acute exacerbation of interstitial pneumonia after surgery for lung cancer. *BMC Pulmonary Medicine* 2021; 21: 186.
48. Qin H-Y, Li M-D, Xie G-F, Cao W, Xu D-X, Zhao H, Fu L. Associations among S100A4, Sphingosine-1-Phosphate, and Pulmonary Function in Patients with Chronic Obstructive Pulmonary Disease. *Oxidative Medicine and Cellular Longevity* 2022; 2022: 6041471.
49. Ruffenach G, Hong J, Vaillancourt M, Medzikovic L, Eghbali M. Pulmonary hypertension secondary to pulmonary fibrosis: clinical data, histopathology and molecular insights. *Respiratory Research* 2020; 21: 303.
50. Ackermann M, Stark H, Neubert L, Schubert S, Borchert P, Linz F, Wagner WL, Stiller W, Wielpütz M, Hoefer A, Haverich A, Mentzer SJ, Shah HR, Welte T, Kuehnel M, Jonigk D. Morphomolecular motifs of pulmonary neoangiogenesis in interstitial lung diseases. *The European respiratory journal* 2020; 55.

Table 1: subject demographics and clinical characteristics

	Normal Control (NC)	**IPF**
Factor	Values *	
Total Number (n)	15	13
Age	44 ± 20.1	64 ± 5.06
Gender (F/M)	6/5	6/7
Body Mass Index	NA	26.69 ± 3.03
Smoking Status: Current, Ex-smoker and Never (n)	non-smokers	0/7/6
Smoking pack-years	-	20.84 ± 23.16
Lung physiology		
FEV_1 (L)	-	1.70 ±0.40
FEV_1 (%) Predicted	-	60.17 ±12.22
FVC (L)	-	1.97±0.51
FVC (%) Predicted	-	53.5±12.98
DLCO (ml/min/mmHg)	-	5.91±2.92
DLCO Corrected (%) Predicted	-	25.85±15.30

*Values represents the mean and the standard deviation; NA- not available

Table 2: Correlation analysis-mesenchymal markers vs arterial thickness and lung function

Correlation Analysis		
a) Arterial Thickness	**Intimal N-cadherin**	**Intimal Vimentin**
Intima	**r'= 0.64 p=0.01**	**r'= 0.60 p=0.03**
Media	**r'= 0.12 p=0.36**	**r'= 0.10 p=0.38**
Adventitia	**r'= 0.28 p=0.19**	**r'= 0.25 p=0.22**
b) Lung Function		
FEV1 (L)	**r'= -0.40 p=0.09**	**r'= 0.05 p=0.44**
FVC (L)	**r'= -0.27 p=0.20**	**r'= 0.18 p=0.29**
DLCO (%)	**r'=- 0.58 p=0.04**	**r'= -0.56 p=0.03**

***p=< 0.05* was considered significant**

Figure 1A) Immunohistology stained slides for pulmonary arteries from NC and IPF for VE-Cadherin **a)** 100-199µm (20x magnification), **b)** 200-399µm (20x magnification), **c)** 400-599µm (20x magnification) and **d)** 600-1000µm (10x magnification).

Figure 1B) Immunohistology stained slides for pulmonary arteries from NC and IPF for N-Cadherin **a)** 100-199µm (20x magnification), **b)** 200-399µm (20x magnification), **c)** 400-599µm (20x magnification) and **d)** 600-1000µm (10x magnification).

Figure 1C) Immunohistology stained slides for pulmonary arteries from NC and IPF for vimentin **a)** 100-199µm (20x magnification), **b)** 200-399µm (20x magnification), **c)** 400-599µm (20x magnification) and **d)** 600-1000µm (10x magnification).

Figure 1D) Immunohistology stained slides for pulmonary arteries from NC and IPF for S100A4 **a)** 100-199µm (20x magnification), **b)** 200-399µm (20x magnification), **c)** 400-599µm (20x magnification) and **d)** 600-1000µm (10x magnification).

Figure 2A) Percent expression of VE -cadherin and N-cadherin positive cells in intimal layer in IPF and NC across arterial size 100-1000µm **a)** VE-cadherin junctional positive **b)** VE-cadherin cytoplasmic positive **c)** N-cadherin junctional positive **d)** N-cadherin cytoplasmic positive.

Figure 2B) VE- cadherin and N-cadherin positive cells ratio in IPF and NC **e)** VE-cadherin junctional positive vs N-cadherin junctional positive **f)** VE-cadherin cytoplasmic positive vs N-cadherin cytoplasmic positive. All data are presented as multiple comparisons with Ordinary one-way ANOVA; $p \leq 0.05$ was considered significant.

Figure 3) N-cadherin expression in NC and IPF **a**) total arterial N-cadherin expression across arterial size 100-1000µm **b)** 100-199µm, **c)** 200-399µm, **d)** 400-599µm and **e)** 600-1000µm. All data are presented as multiple comparisons with Ordinary one-way ANOVA; $p \leq 0.05$ was considered significant.

Figure 4) Vimentin Expression in NC and IPF **a**) total arterial vimentin expression across arterial size 100-1000µm **b)** 100-199µm, **c)** 200-399µm, **d)** 400-599µm and **e)** 600-1000µm. All data are presented as multiple comparisons with Ordinary one-way ANOVA; $p \leq 0.05$ was considered significant.

Figure 5) S100A4 expression in NC and IPF **a**) total arterial vimentin expression across arterial size 100-1000µm **b)** 100-199µm, **c)** 200-399µm, **d)** 400-599µm and **e)** 600-1000µm. All data are presented as multiple comparisons with Ordinary one-way ANOVA; $p \leq 0.05$ was considered significant.

Figure 6) Correlations between **a)** total N-cadherin percent expression and vs total arterial thickness **b)** total vimentin percent expression and vs total arterial thickness **c)** total N-cadherin percent expression vs % DLCO and **d)** total vimentin percent expression and vs % DLCO.

Figure 7A) CD4, CD8 and mast cell chymase (CMA1) staining in arterial layers of NC and patients with IPF. Images were taken at 40x magnification.

Figure 7B) Neutrophil elastase (NE), CD68 and PDGFR-β staining in arterial layers of NC and patients with IPF. Images were taken at 40x magnification, and the insert image was taken at 100x with a bright field.

Supplementary Figure 1) VE-cadherin measurement strategy in NC and IPF (40X magnification). **b)** N-cadherin measurement strategy in NC and IPF (40X magnification). In figure, basement membrane thickness measurement (Z), using two reference lines: one at basement membrane(X) and outer endothelium (Y) were drawn using automated software Image-Pro Plus and the average distance (µm) between two lines were measured. In figure, represents junctional positive cells * represent cytoplasmic positive cells and represents the distance between two reference line X and Y **c)** Arterial layer mesenchymal measurement strategy in NC and IPF. Total arterial mesenchymal expression was measured by selecting total arterial circumference. In the inset are various layers (T1- Intima, T2- Media and T3- Adventitia) mesenchymal expression.

Supplementary Figure 2) Pearson coefficient correlations between VE-cadherin expression and mesenchymal marker expression in IPF across arterial size **a)** 100-199µm, **b)** 200-399µm, **c)** 400-599µm and **d)** 600-1000µm.

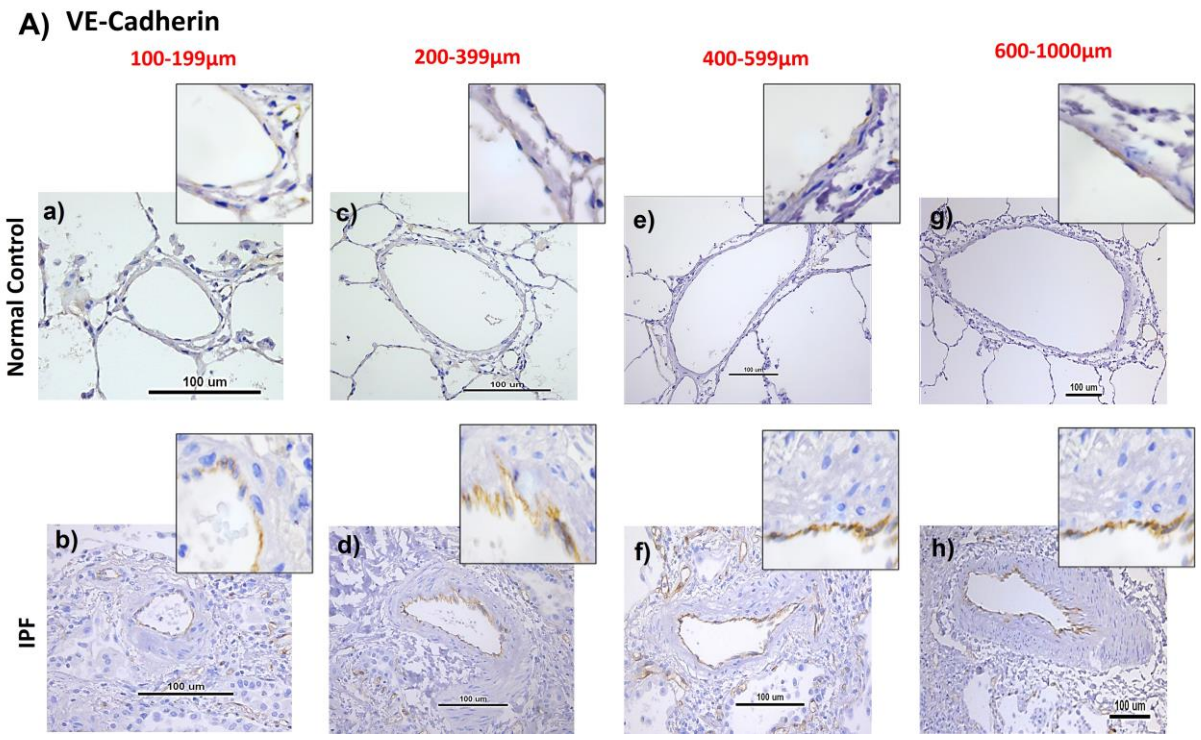
A) VE-Cadherin
100-199µm
200-399µm
400-599µm
600-1000µm
Normal Control
IPF
a)
b)
c)
d)
e)
f)
g)
h)
100 um

B) N-Cadherin

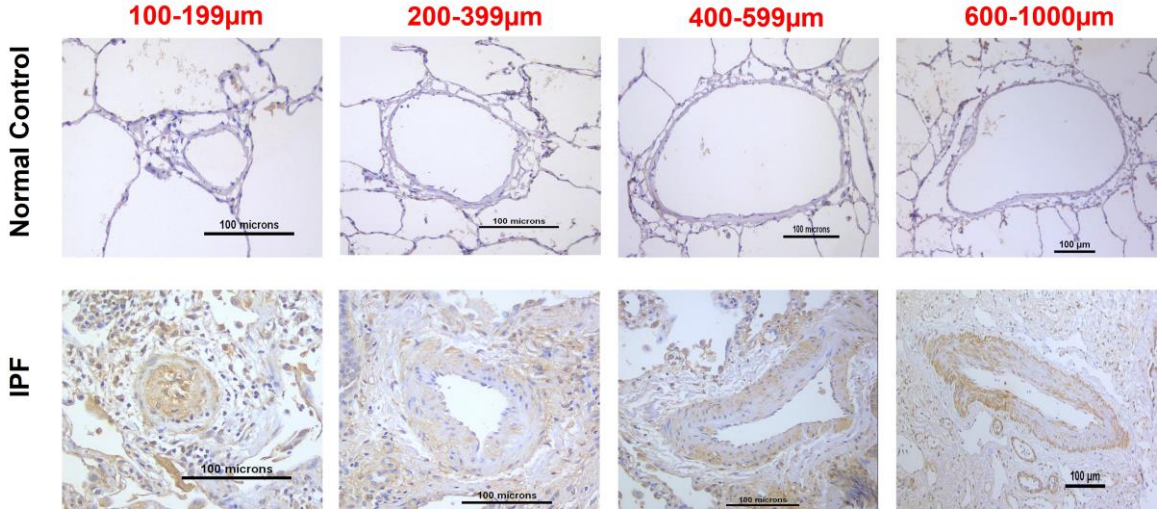

B) N-Cadherin

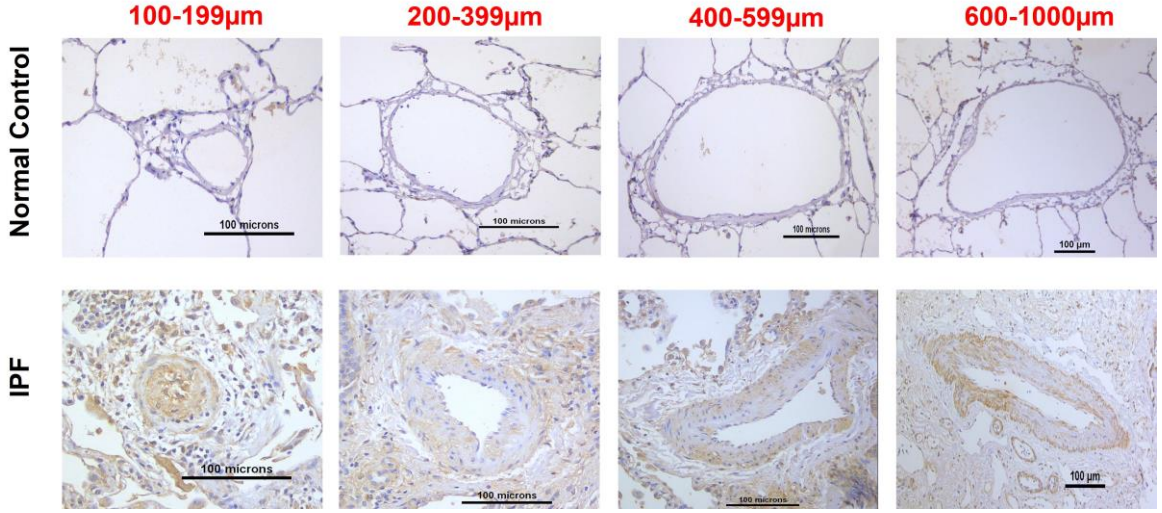

C) Vimentin

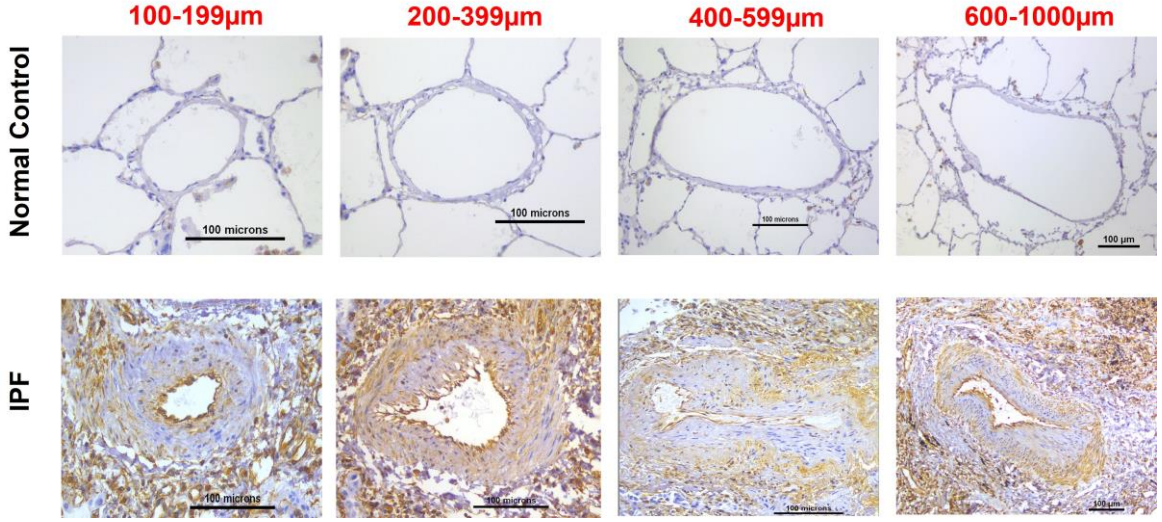

D) S100A4

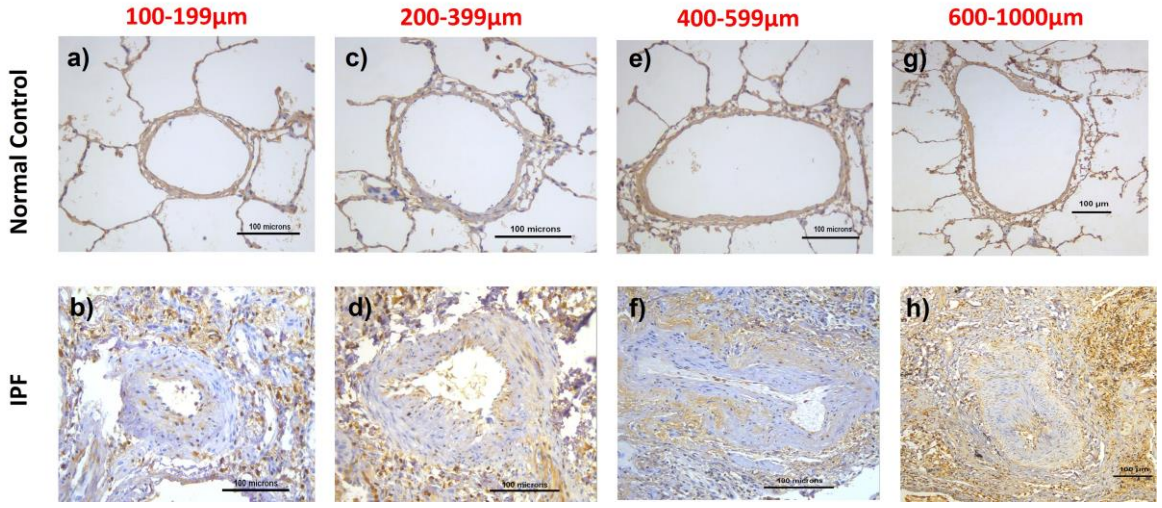
100-199µm
200-399µm
400-599µm
600-1000µm
Normal Control
IPF
a)
b)
c)
d)
e)
f)
g)
h)
100 microns
100 µm

A)

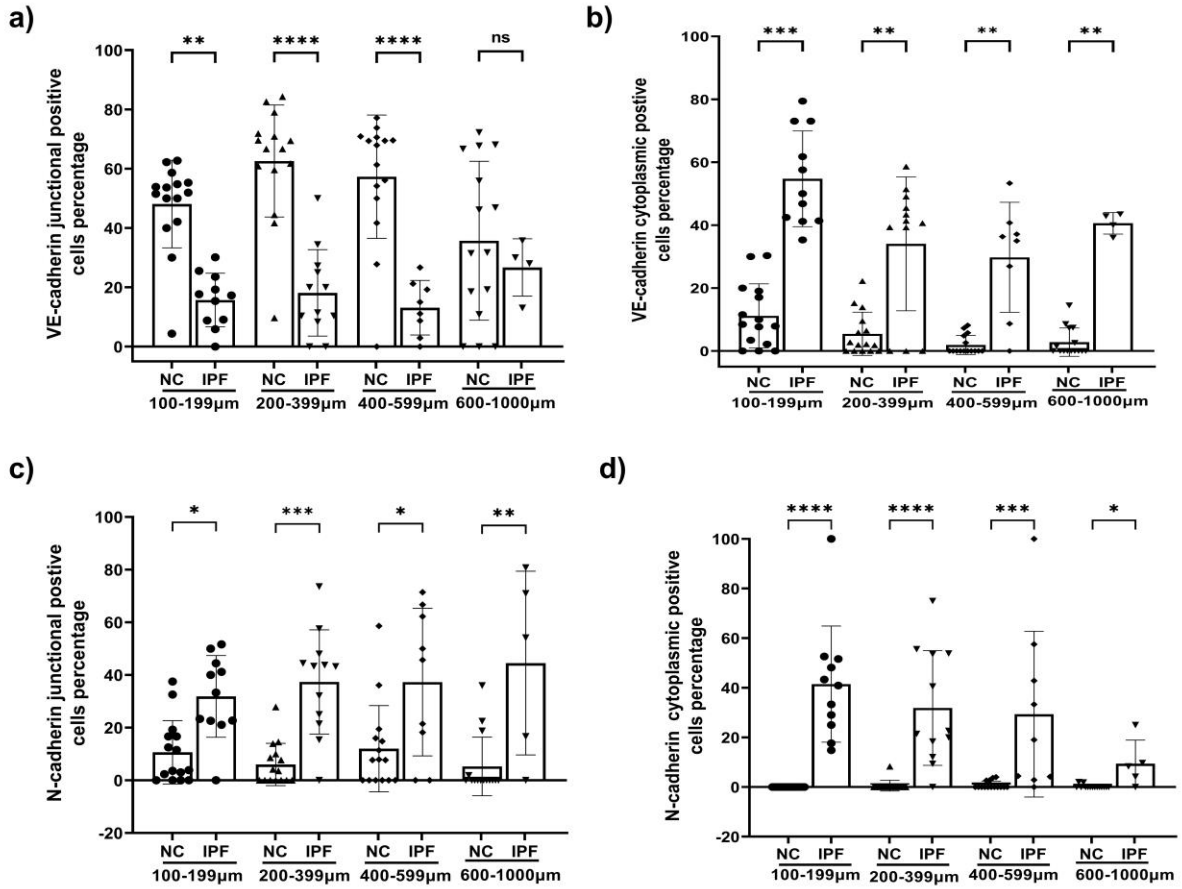
a)
VE-cadherin junctional positive cells percentage
**
****
****
ns
NC IPF
100-199µm
200-399µm
400-599µm
600-1000µm
b)
VE-cadherin cytoplasmic postive cells percentage
***
**
**
**
c)
N-cadherin junctional postive cells percentage
*
***
*
**
d)
N-cadherin cytoplasmic positive cells percentage
****
****
***
*

B)

a)

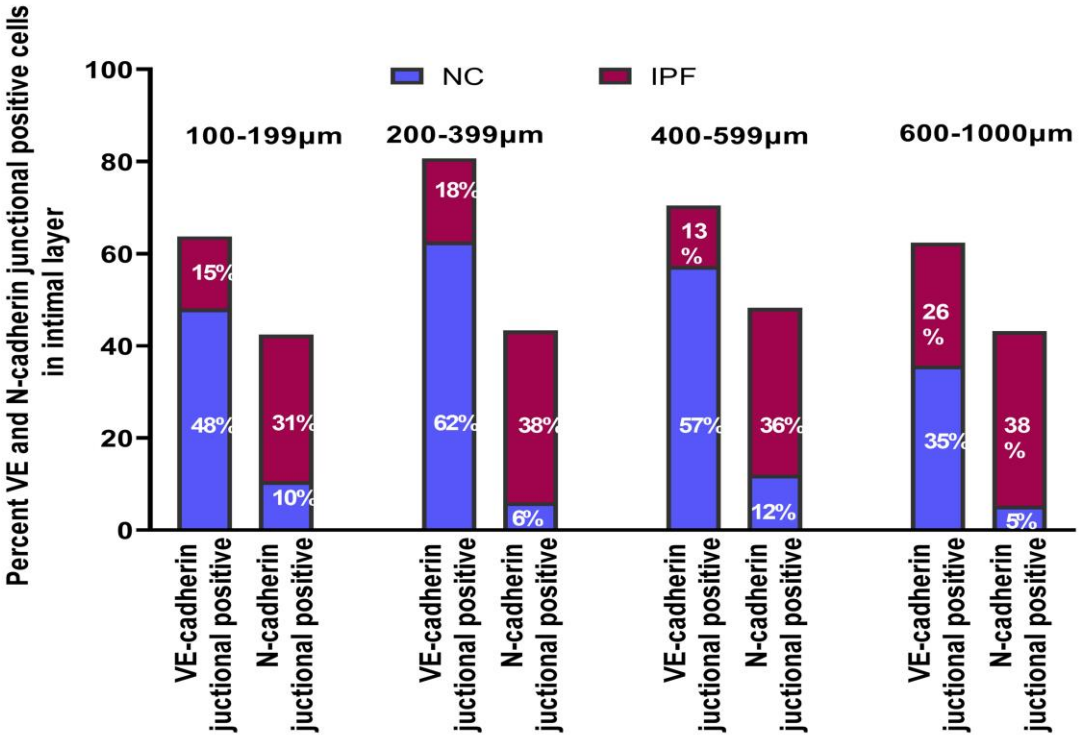
Percent VE and N-cadherin junctional positive cells in intimal layer
NC
IPF
100-199µm
200-399µm
400-599µm
600-1000µm
100
80
60
40
20
0
15%
48%
31%
10%
18%
62%
38%
6%
13 %
57%
36%
12%
26 %
35%
38 %
5%
VE-cadherin juctional positive
N-cadherin juctional positive
VE-cadherin juctional positive
N-cadherin juctional positive
VE-cadherin juctional positive
N-cadherin juctional positive
VE-cadherin juctional positive
N-cadherin juctional positive

b)

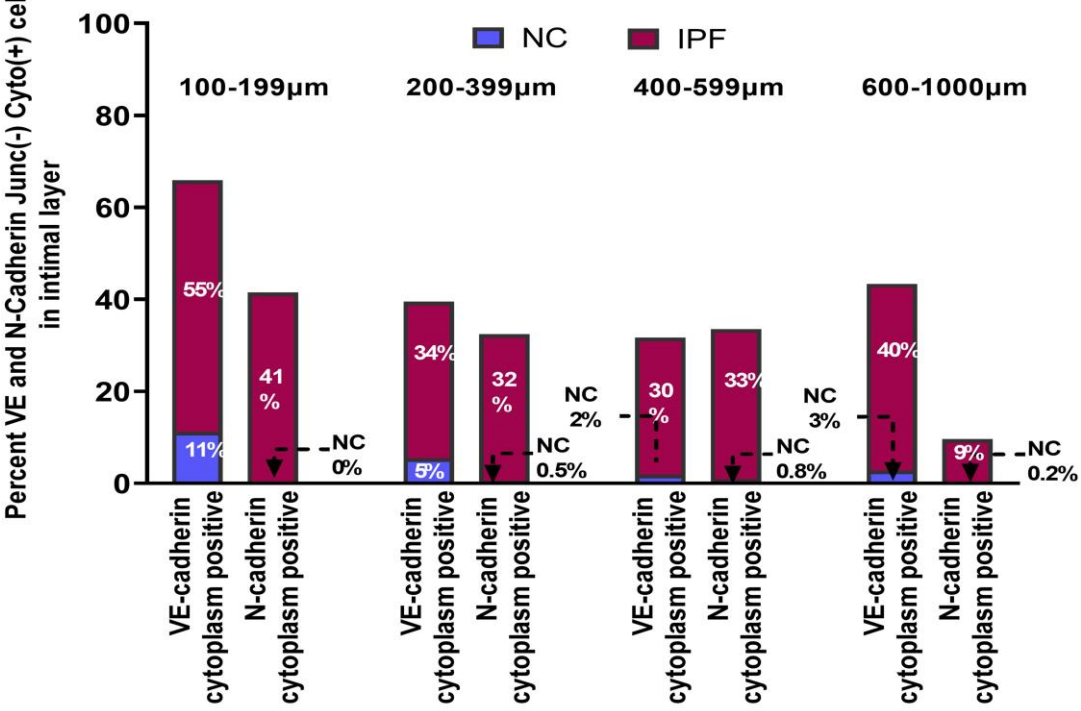
Percent VE and N-Cadherin Junc(-) Cyto(+) cells in intimal layer
NC
IPF
100-199µm
200-399µm
400-599µm
600-1000µm
100
80
60
40
20
0
55%
11%
41 %
NC 0%
34%
5%
32 %
NC 0.5%
NC 2%
30 %
33%
NC 0.8%
NC 3%
40%
9%
NC 0.2%
VE-cadherin cytoplasm positive
N-cadherin cytoplasm positive
VE-cadherin cytoplasm positive
N-cadherin cytoplasm positive
VE-cadherin cytoplasm positive
N-cadherin cytoplasm positive
VE-cadherin cytoplasm positive
N-cadherin cytoplasm positive

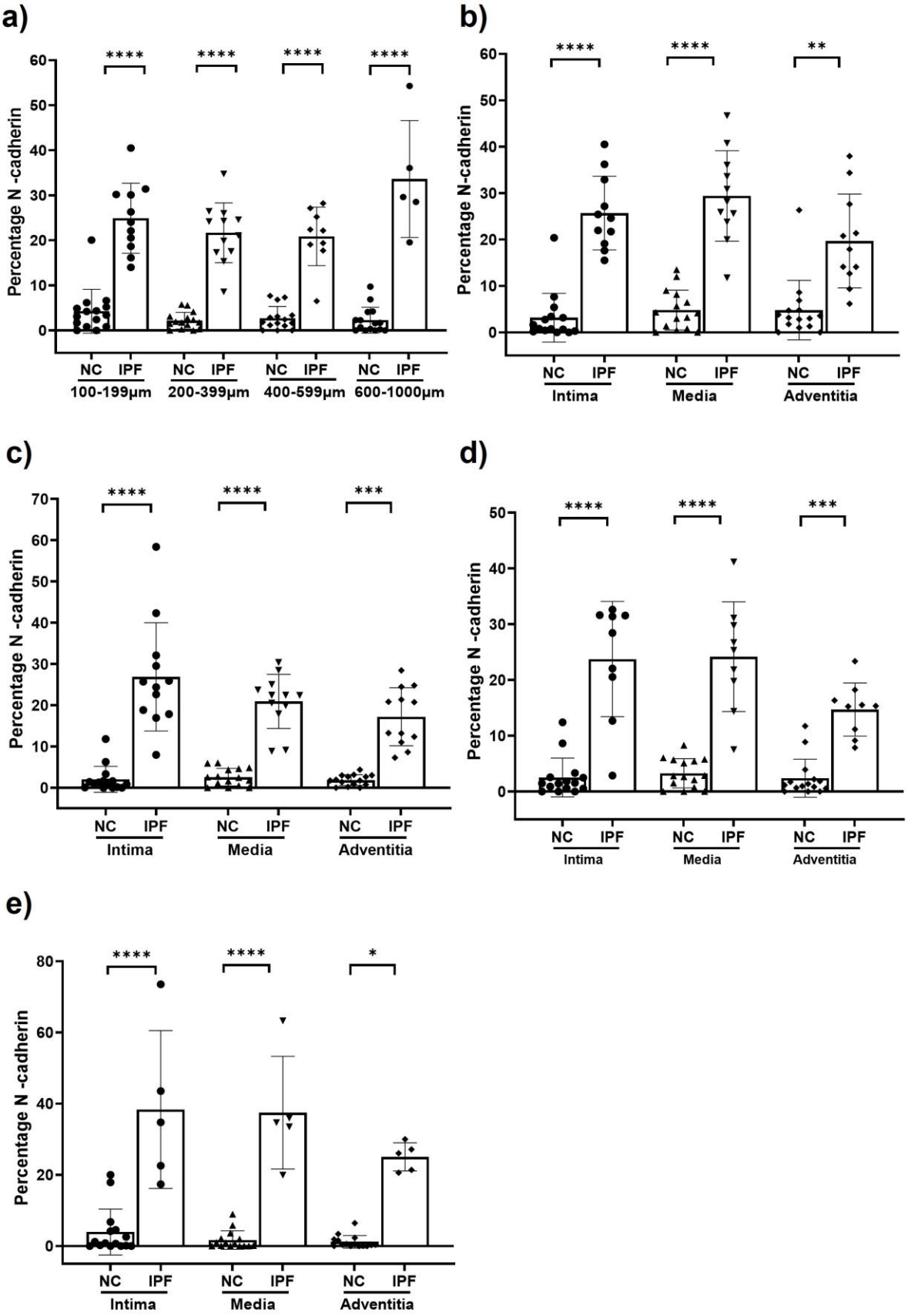
a)
Percentage N -cadherin
****
****
****
****
NC IPF
100-199µm
NC IPF
200-399µm
NC IPF
400-599µm
NC IPF
600-1000µm
b)
Percentage N-cadherin
****
****
**
NC IPF
Intima
NC IPF
Media
NC IPF
Adventitia
c)
Percentage N -cadherin
****
****
***
NC IPF
Intima
NC IPF
Media
NC IPF
Adventitia
d)
Percentage N -cadherin
****
****
***
NC IPF
Intima
NC IPF
Media
NC IPF
Adventitia
e)
Percentage N -cadherin
****
****
*
NC IPF
Intima
NC IPF
Media
NC IPF
Adventitia

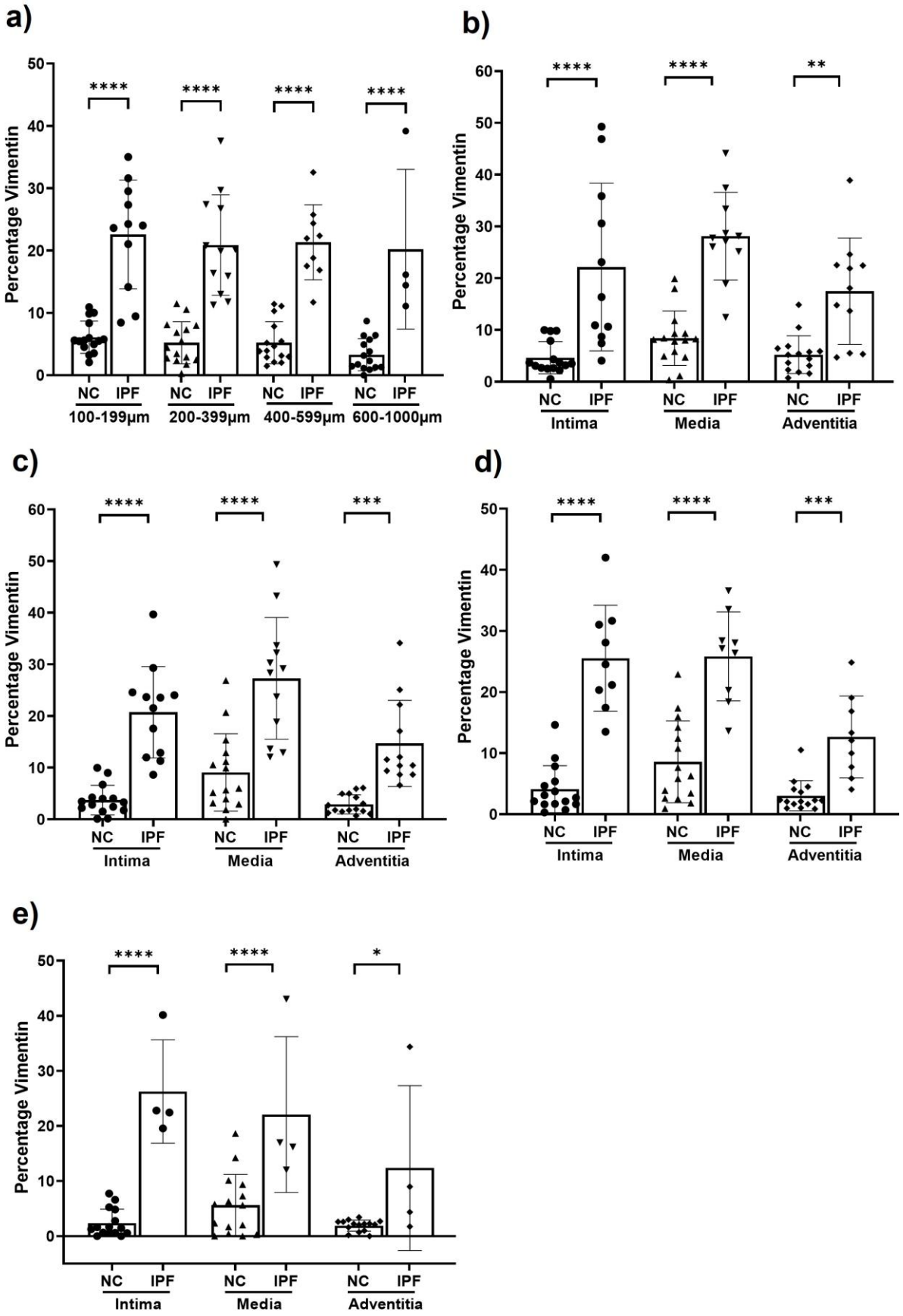
a)
Percentage Vimentin
****
****
****
****
NC IPF
100-199μm
NC IPF
200-399μm
NC IPF
400-599μm
NC IPF
600-1000μm
b)
Percentage Vimentin
****
****
**
NC IPF
Intima
NC IPF
Media
NC IPF
Adventitia
c)
Percentage Vimentin
****
****
***
NC IPF
Intima
NC IPF
Media
NC IPF
Adventitia
d)
Percentage Vimentin
****
****
***
NC IPF
Intima
NC IPF
Media
NC IPF
Adventitia
e)
Percentage Vimentin
****
****
*
NC IPF
Intima
NC IPF
Media
NC IPF
Adventitia

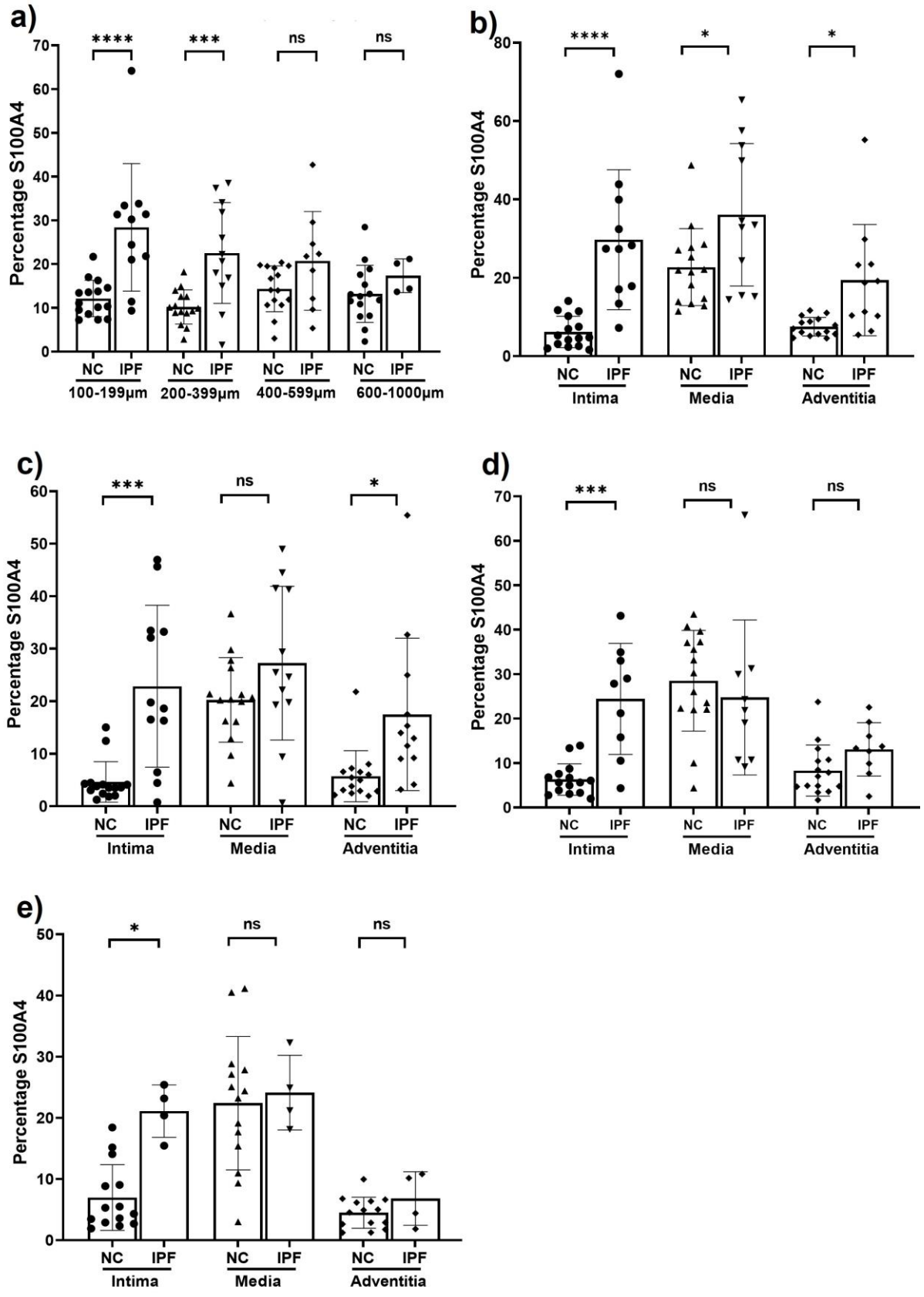
a)
Percentage S100A4
****
***
ns
ns
NC IPF
100-199μm
200-399μm
400-599μm
600-1000μm
b)
Percentage S100A4
****
*
*
NC IPF
Intima
Media
Adventitia
c)
Percentage S100A4
***
ns
*
NC IPF
Intima
Media
Adventitia
d)
Percentage S100A4
***
ns
ns
NC IPF
Intima
Media
Adventitia
e)
Percentage S100A4
*
ns
ns
NC IPF
Intima
Media
Adventitia

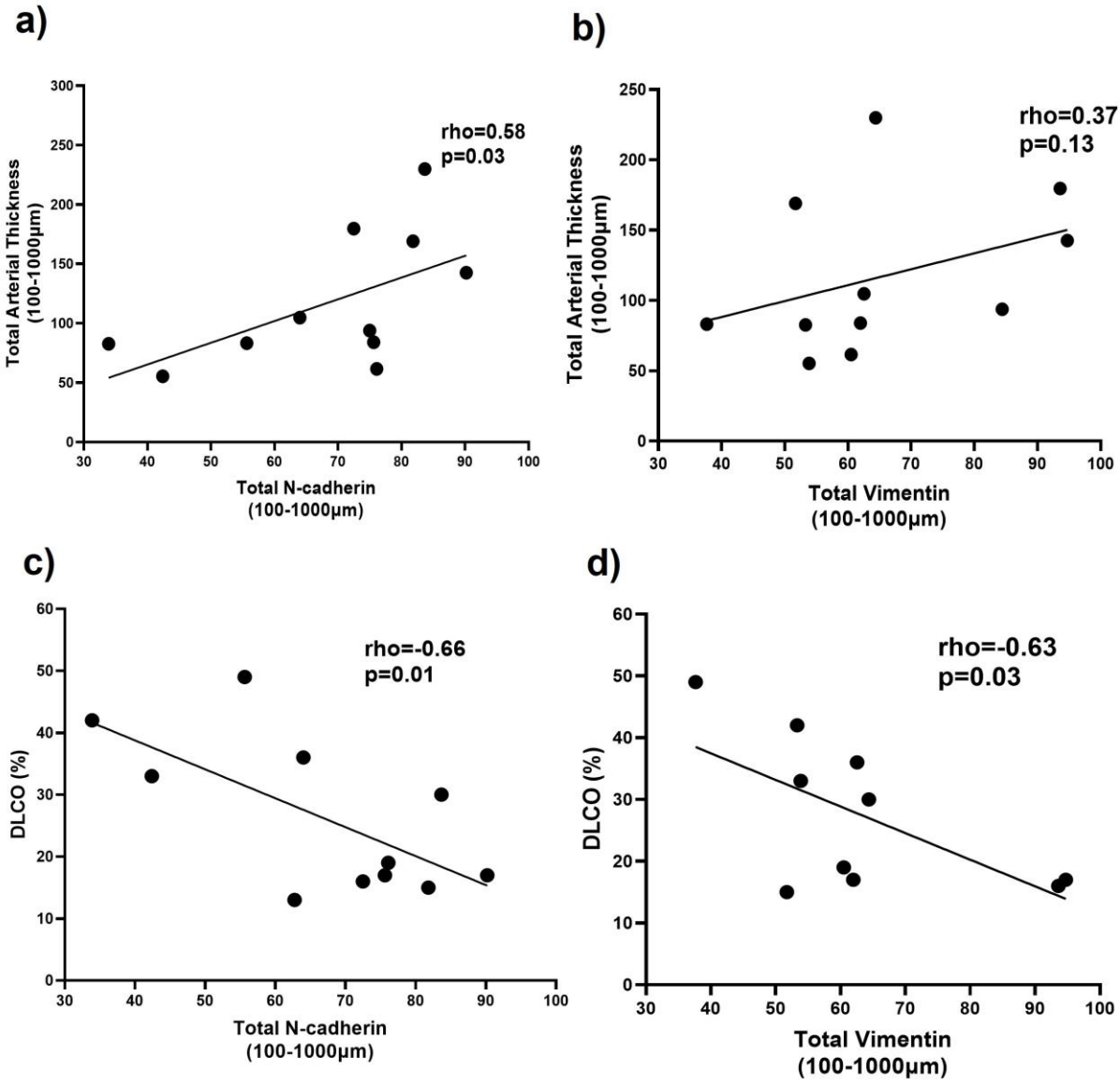
a)
rho=0.58
p=0.03
Total Arterial Thickness (100-1000µm)
Total N-cadherin (100-1000µm)
b)
rho=0.37
p=0.13
Total Arterial Thickness (100-1000µm)
Total Vimentin (100-1000µm)
c)
rho=-0.66
p=0.01
DLCO (%)
Total N-cadherin (100-1000µm)
d)
rho=-0.63
p=0.03
DLCO (%)
Total Vimentin (100-1000µm)

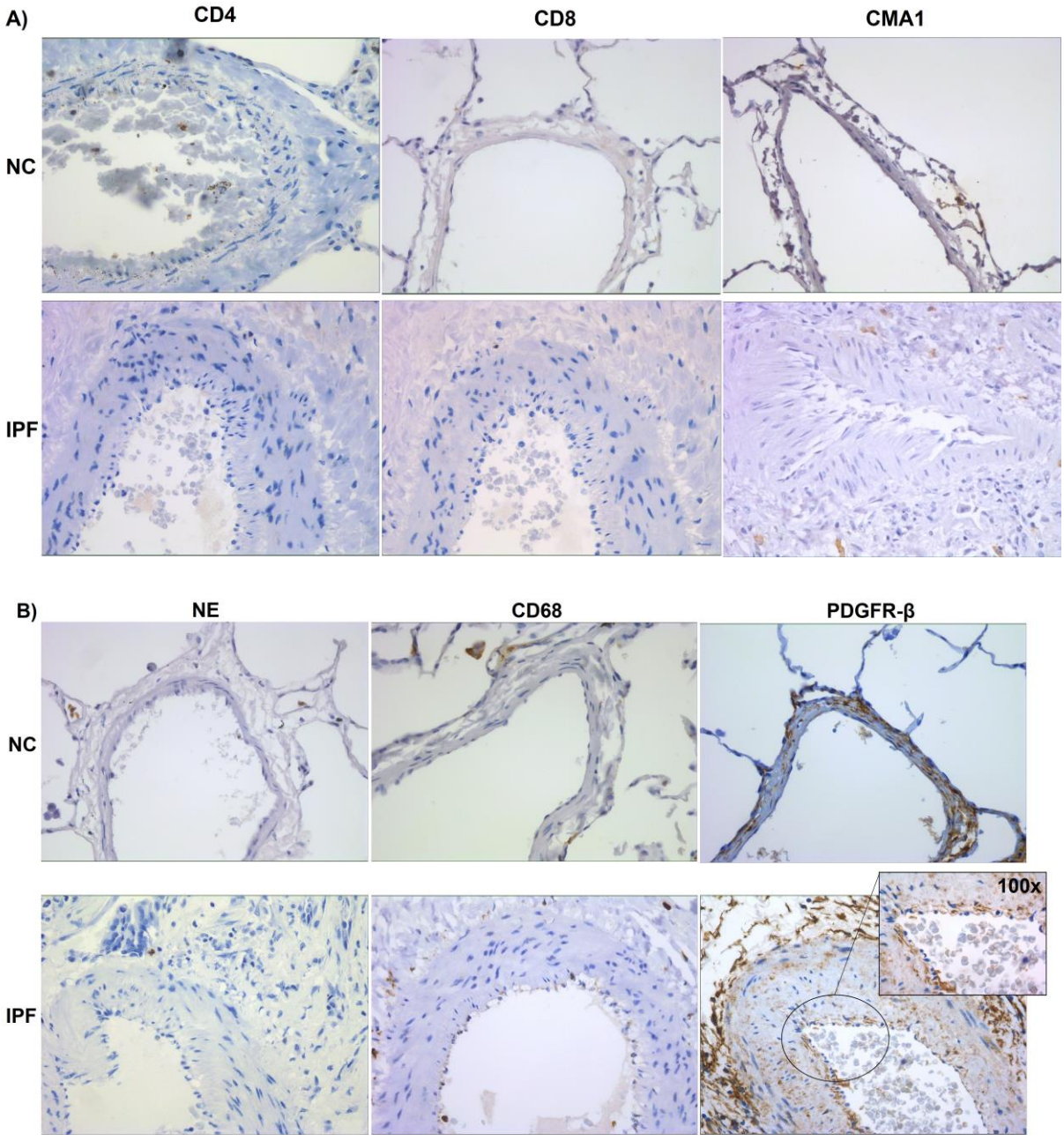
A)
CD4
CD8
CMA1
NC
IPF
B)
NE
CD68
PDGFR-β
NC
IPF
100x

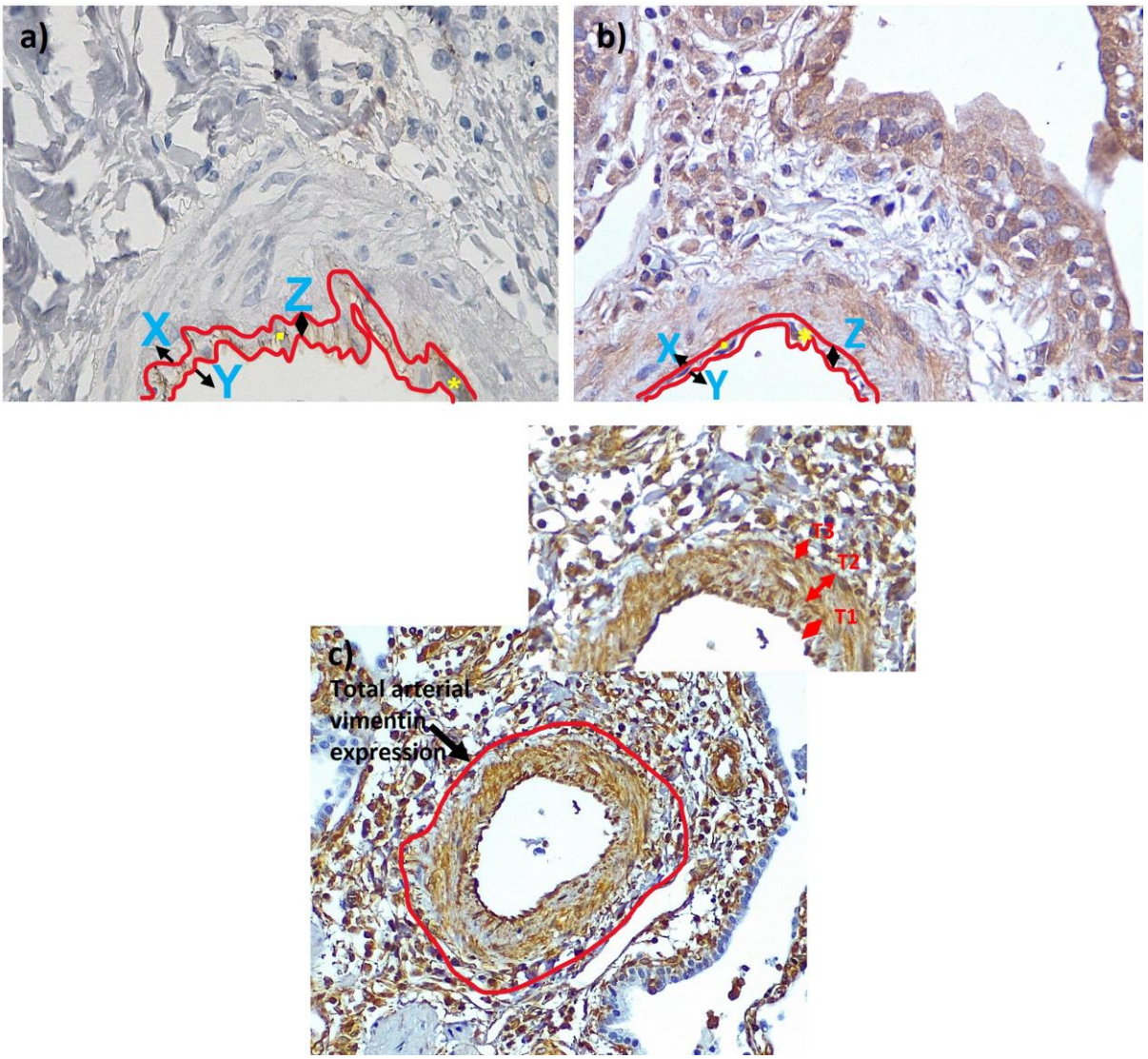
a)
X
Y
Z
b)
X
Y
Z
T3
T2
T1
c)
Total arterial
vimentin
expression

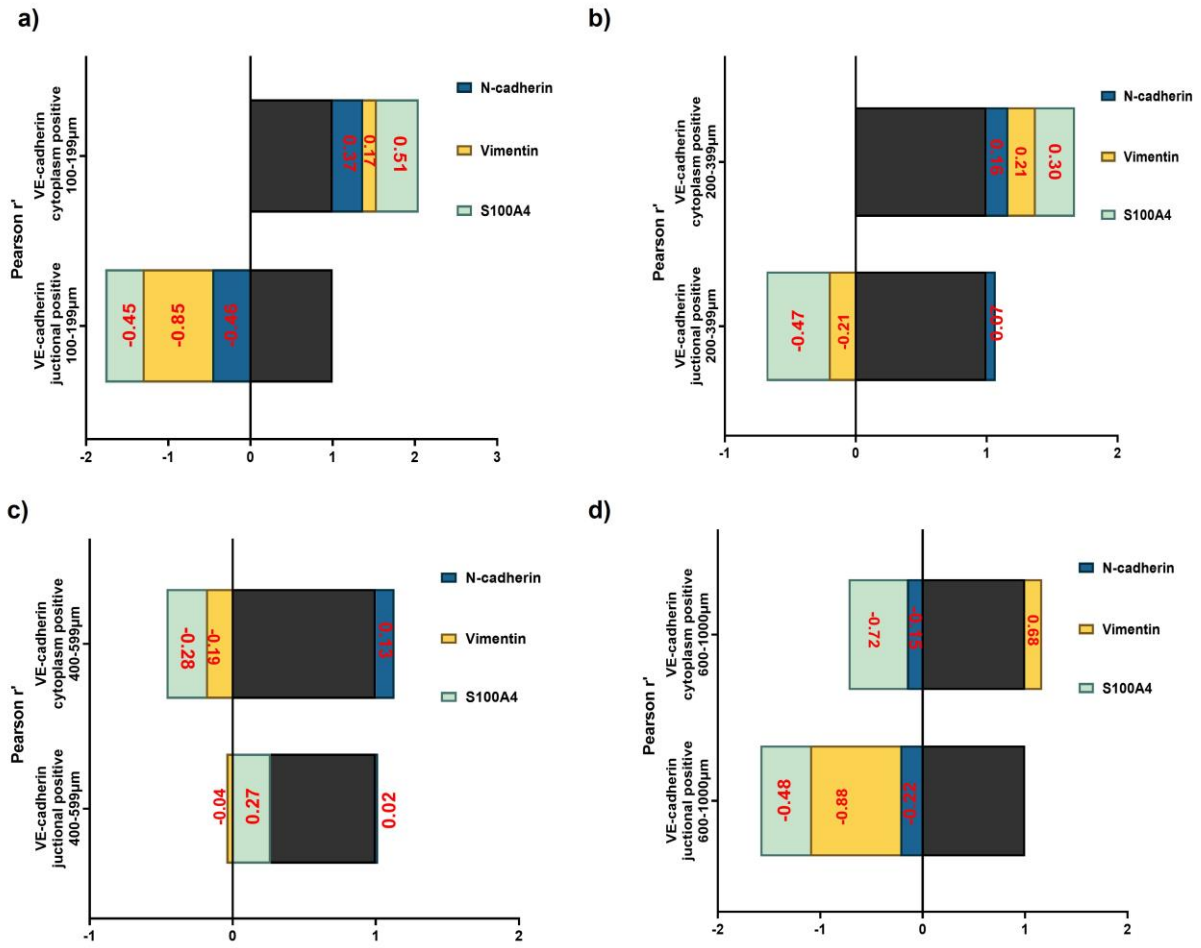
a)
Pearson r'
VE-cadherin cytoplasm positive 100-199µm
VE-cadherin juctional positive 100-199µm
N-cadherin
Vimentin
S100A4
0.37
0.17
0.51
-0.45
-0.85
-0.46
-2
-1
0
1
2
3
b)
Pearson r'
VE-cadherin cytoplasm positive 200-399µm
VE-cadherin juctional positive 200-399µm
N-cadherin
Vimentin
S100A4
0.16
0.21
0.30
-0.47
-0.21
0.10
-1
0
1
2
c)
Pearson r'
VE-cadherin cytoplasm positive 400-599µm
VE-cadherin juctional positive 400-599µm
N-cadherin
Vimentin
S100A4
-0.28
-0.16
0.13
-0.04
0.27
0.02
-1
0
1
2
d)
Pearson r'
VE-cadherin cytoplasm positive 600-1000µm
VE-cadherin juctional positive 600-1000µm
N-cadherin
Vimentin
S100A4
-0.72
-0.11
0.68
-0.48
-0.88
-2
-1
0
1
2